

More About This Article

Additional resources and features associated with this article are available within the HTML version:

- Supporting Information
- Links to the 4 articles that cite this article, as of the time of this article download
- Access to high resolution figures
- Links to articles and content related to this article
- Copyright permission to reproduce figures and/or text from this article

[View the Full Text HTML](#)

## Chemical Tuning of Positive and Negative Magnetoresistances, and Superconductivity in 1222-Type Ruthenocuprates

Abbie C. McLaughlin,<sup>\*,†</sup> Laura Begg,<sup>†</sup> Catriona Harrow,<sup>†</sup> Simon A. J. Kimber,<sup>§</sup> Falak Sher,<sup>§,¶</sup> and J. Paul Attfield<sup>\*,§</sup>

The Chemistry Department, University of Aberdeen, Meston Walk, Aberdeen AB24 3UE, United Kingdom, and Centre for Science at Extreme Conditions and School of Chemistry, University of Edinburgh, King's Buildings, Mayfield Road, Edinburgh EH9 3JZ, United Kingdom

Received July 5, 2006; E-mail: a.c.mclaughlin@abdn.ac.uk; j.p.attfield@ed.ac.uk

High critical-temperature superconductivity and large ("colossal") magnetoresistances are two important electronic conducting phenomena found in transition metal oxides. High- $T_c$  materials have applications such as superconducting magnets for MRI and NMR, and magnetoresistive materials may find use in magnetic sensors and spintronic devices. Here we report chemical doping studies of  $\text{RuSr}_2(\text{R}_{2-x}\text{Ce}_x)\text{Cu}_2\text{O}_{10-\delta}$  ruthenocuprates which show that a single oxide system can be tuned between superconductivity at high hole dopings and varied magnetoresistive properties at low doping levels. A robust variation of negative magnetoresistance with hole concentration is found in the  $\text{RuSr}_2\text{R}_{1.8-x}\text{Y}_{0.2}\text{Ce}_x\text{Cu}_2\text{O}_{10-\delta}$  series, while  $\text{RuSr}_2\text{R}_{1.1}\text{Ce}_{0.9}\text{Cu}_2\text{O}_{10-\delta}$  materials show an unprecedented crossover from negative to positive magnetoresistance with rare earth ( $R$ ) ion radius.

Although the mechanism for superconductivity in layered cuprates remains controversial,<sup>1</sup> the chemical tuning of their properties is well established. Oxidation of the  $\text{CuO}_2$  planes suppresses antiferromagnetic order of  $\text{Cu}^{2+}$   $S = 1/2$  spins and induces superconductivity in the doping range  $p = 0.06-0.25$  (the equivalent Cu oxidation states are  $2+p$ ). Ruthenocuprates contain distinct  $\text{RuO}_2$  and  $\text{CuO}_2$  planes and display coexisting ferromagnetism and superconductivity in both 1212-type ( $\text{RuSr}_2\text{RCu}_2\text{O}_8$ )<sup>2,3</sup> and 1222-type ( $\text{RuSr}_2(\text{R,Ce})_2\text{Cu}_2\text{O}_{10-\delta}$ )<sup>4,5</sup> structures, where  $R = \text{Sm, Eu, or Gd}$ . Large negative magnetoresistances (change of electrical resistivity  $\rho$  in an applied magnetic field  $H$ , defined as  $\text{MR} = (\rho(H) - \rho(0))/\rho(0)$ ) have recently been observed in nonsuperconducting  $R = (\text{Nd, Y})$  1222 materials,<sup>6</sup> up to  $\text{MR} = -34\%$  for  $\text{RuSr}_2\text{NdY}_{0.1}\text{Ce}_{0.9}\text{Cu}_2\text{O}_{10-\delta}$  at 4 K and 7 T. The results presented here reveal an exquisite chemical tuning of the properties of 1222 ruthenocuprates between superconducting and magnetoresistive properties, including a previously unreported, large positive magnetoresistance state.

1222-type ruthenocuprates contain metal oxide layers in the repeat sequence;  $\cdots\text{RuO}_2\cdot\text{SrO}\cdot\text{CuO}_2\cdot(\text{R,Ce})\cdot\text{O}_{2-\delta}\cdot(\text{R,Ce})\cdot\text{CuO}_2\cdot\text{SrO}\cdots$  (Table of Contents graphic shows the crystal structure). The chemistry of the  $(\text{R,Ce})_2\text{O}_{2-\delta}$  slab between the two  $\text{CuO}_2$  planes controls the electronic properties. Two series of polycrystalline ceramic 1222 samples,  $\text{RuSr}_2\text{Nd}_{1.8-x}\text{Y}_{0.2}\text{Ce}_x\text{Cu}_2\text{O}_{10-\delta}$  ( $0.70 < x < 0.95$ ) and  $\text{RuSr}_2\text{R}_{1.1}\text{Ce}_{0.9}\text{Cu}_2\text{O}_{10-\delta}$  ( $R_{1.1} = \text{Nd}_{1.0}\text{Y}_{0.1}, \text{Nd}_{0.9}\text{Y}_{0.2}, \text{Sm}_{1.1}, \text{Sm}_{0.9}\text{Y}_{0.2}, \text{Eu}_{0.9}\text{Y}_{0.2}, \text{Gd}_{0.9}\text{Y}_{0.2}$ ; in order of decreasing radius), have been prepared to determine the respective effects of variable doping and  $R$  cation size.<sup>7</sup> Nd-based 1222 materials only form in a  $\sim 10$  °C synthesis window around 1025 °C and are difficult to prepare pure. A small degree of Y substitution was used to improve phase purity, although  $\sim 5\%$  of a 1212 secondary phase was still present. Phase purity in the  $\text{RuSr}_2\text{R}_{1.1}\text{Ce}_{0.9}\text{Cu}_2\text{O}_{10-\delta}$  series improved with

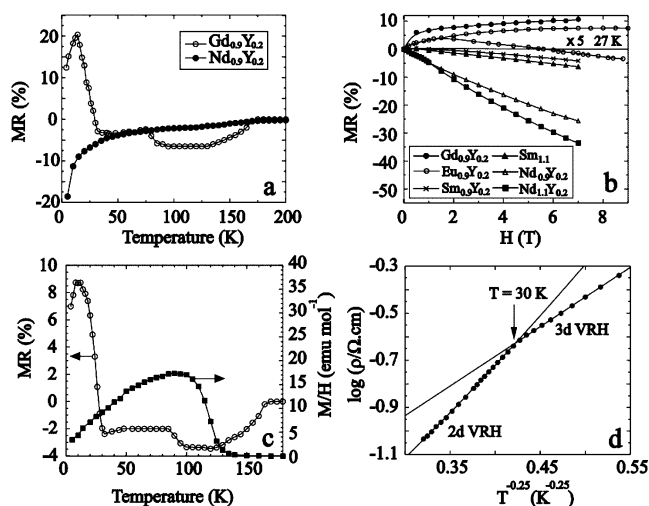


**Figure 1.** Results for  $\text{RuSr}_2\text{R}_{1.1}\text{Ce}_{0.9}\text{Cu}_2\text{O}_{10-\delta}$  materials. (a) MR in a  $H = 5$  T field for two representative samples. (b) MR variations with field at 4 K for all samples; also for  $R_{1.1} = \text{Eu}_{0.9}\text{Y}_{0.2}$  at 27 K, scaled  $\times 5$ . (c) Temperature variations of MR ( $H = 5$  T) and magnetic susceptibility ( $H = 0.01$  T) for  $R_{1.1} = \text{Eu}_{0.9}\text{Y}_{0.2}$ . (d) Plot of  $\log(\text{resistivity})$  against  $T^{-1/4}$  for  $R_{1.1} = \text{Eu}_{0.9}\text{Y}_{0.2}$  between 12 and 95 K, showing the change from 3-D to 2-D variable range hopping conductivity at 30 K.

decreasing  $R$  size; the  $R_{1.1} = \text{Eu}_{0.9}\text{Y}_{0.2}$  and  $\text{Gd}_{0.9}\text{Y}_{0.2}$  materials were phase pure by powder X-ray diffraction.

Portions of high (low)  $x$   $\text{RuSr}_2\text{Nd}_{1.8-x}\text{Y}_{0.2}\text{Ce}_x\text{Cu}_2\text{O}_{10-\delta}$  samples were annealed under flowing  $\text{N}_2$  at 600 °C ( $\text{O}_2$  at 800 °C) for 10 h and cooled at  $2$  °C $\cdot\text{min}^{-1}$  to increase (decrease) the oxygen deficiency  $\delta$  and thereby extend the available hole-doping range. Precise oxygen stoichiometries were determined by thermogravimetric reduction under 5%  $\text{H}_2$  in  $\text{N}_2$ . Ru is known to be in the +5 state in 1222 materials from previous XANES and doping studies,<sup>8</sup> giving  $p = (1 - x - 2\delta)/2$ . Ten  $\text{RuSr}_2\text{Nd}_{1.8-x}\text{Y}_{0.2}\text{Ce}_x\text{Cu}_2\text{O}_{10-\delta}$  samples were synthesized, with  $0.70 < x < 0.95$  and  $0.004 < \delta < 0.095$ , giving a doping range  $0.010 < p < 0.059$  that spans the presuperconducting region for cuprates. Further sample details are given in Supporting Information.

The  $\text{RuSr}_2\text{Nd}_{1.8-x}\text{Y}_{0.2}\text{Ce}_x\text{Cu}_2\text{O}_{10-\delta}$  materials are semiconducting with band gaps of 30–170 meV, and the Cu spins order antiferromagnetically at 25–115 K. The magnetoresistance properties are typified by the data for the  $x = 0.9$  sample in Figure 1a and b. Negative MR is observed below the Ru spin ordering transition  $\sim 160$  K, diverging to large values below the Cu spin ordering temperature of 60 K, and the 4 K MR varies near-linearly with magnetic field. These properties are characteristic of charge transport by magnetopolarons—small ferromagnetic regions surrounding each Cu-hole within a matrix of antiferromagnetically

<sup>†</sup> University of Aberdeen.

<sup>§</sup> University of Edinburgh.

<sup>¶</sup> New address: Pakistan Institute of Engineering and Applied Sciences, Nilore, Islamabad, Pakistan.

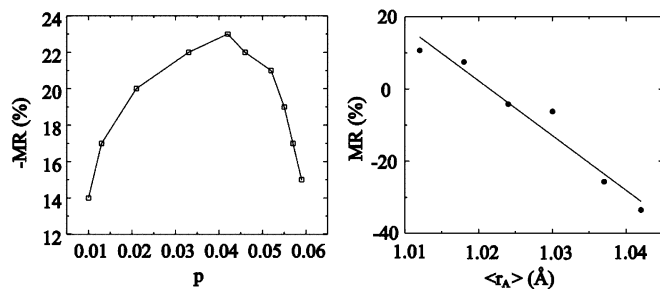


**Figure 2.** (Left) Variation of the  $-MR_{7T}(5\text{ K})$  magnetoresistance with hole doping  $p$  in the  $\text{RuSr}_2\text{Nd}_{1.8-x}\text{Y}_{0.2}\text{Ce}_x\text{Cu}_2\text{O}_{10-\delta}$  series. (Right) Variation of  $MR_{7T}(4\text{ K})$  with  $\langle r_A \rangle$ , the mean  $A$  ( $=\text{R}_{1.1}\text{Ce}_{0.9}$ ) site cation radius.

ordered  $\text{Cu}^{2+}$  spins.<sup>9</sup> An applied magnetic field cants the Ru spins into a ferromagnetic arrangement, which induces partial ferromagnetism in the  $\text{CuO}_2$  planes thereby increasing the mobility of the magnetopolarons, giving the observed, negative MRs.<sup>6</sup> Magnetopolaron hopping is a thermally activated process, leading to a characteristic exponential rise in  $-MR$  below the Cu spin transition,<sup>10</sup> as seen in Figure 1a.

The magnetoresistances in the  $\text{RuSr}_2\text{Nd}_{1.8-x}\text{Y}_{0.2}\text{Ce}_x\text{Cu}_2\text{O}_{10-\delta}$  series (at 4 K and 7 T) show a striking correlation with the doping level  $p$ , as shown in Figure 2. No such MR trend has been reported previously in any cuprate series. Negative MR initially rises with  $p$ , reflecting the increasing number of hole carriers in the  $\text{CuO}_2$  planes, but falls sharply above  $p = 0.04$ . The known onset of superconductivity in ruthenocuprates (and cuprates in general) at  $p > 0.06$ , suggests that this collapse of  $-MR$  corresponds to the onset of hole pairing, as the singlet Cu hole pairs that carry the supercurrent do not contribute to the magnetotransport. Hence, our magnetoresistance data show that superconducting pair formation starts above a distinct threshold concentration of 4% doping, although the coherent superconducting state is observed only for  $>6\%$  doping.

To discover how  $R^{3+}$  cation size influences magnetoresistance at a constant  $R/\text{Ce}$  ratio, a series of  $\text{RuSr}_2\text{R}_{1.1}\text{Ce}_{0.9}\text{Cu}_2\text{O}_{10-\delta}$  samples was prepared. A remarkable change is observed on going from the above  $R = (\text{Nd}, \text{Y})$  materials to the small-radius  $R = (\text{Gd}, \text{Y})$  and  $(\text{Eu}, \text{Y})$  analogues, which show a complex thermal evolution of MR (in Figure 1a and c, respectively). Cooling below the onset of negative MR, a small discontinuity to less negative values is seen at the Cu spin ordering transition at 80 K. This is identified from the susceptibility maximum in Figure 1c,<sup>6</sup> and suggests that the Cu spin structure is different from that in the  $R = (\text{Nd}, \text{Y})$  materials. A sharp transition at 30 K leads to a large positive MR peak of 22% at 10 K for  $R = (\text{Gd}, \text{Y})$ . The low-temperature, positive MR rises rapidly with field, and higher temperature (27 K) measurements show that MR goes through a broad maximum and then decreases to negative values (Figure 1b). The 4 K MRs in the  $\text{RuSr}_2\text{R}_{1.1}\text{Ce}_{0.9}\text{Cu}_2\text{O}_{10-\delta}$  series show an approximately linear cross-over from large positive to negative values with increasing  $R$  cation radius.<sup>11</sup> There is no corresponding correlation between MR and the  $R^{3+}$  paramagnetic moment, confirming that the size effect is dominant. Hence, the 1222 ruthenocuprates show a novel positive to negative MR transition that can be induced by increasing temperature, magnetic field strength, or cation radius. A thermal crossover from negative to positive MR has been reported in  $\text{Zn}_{1-x}\text{Cu}_x\text{Cr}_2\text{Se}_4$  selenides,<sup>12</sup> but the strong size control of the sign of MR found here is unprecedented.

No magnetic anomaly is observed at the 30 K MR discontinuity in  $\text{RuSr}_2\text{Eu}_{0.9}\text{Y}_{0.2}\text{Ce}_{0.9}\text{Cu}_2\text{O}_{10-\delta}$  (Figure 1c); however, a subtle electronic transition is evidenced from a change in the resistivity variation (Figure 1d) from  $\rho \sim \exp(A \cdot T^{-1/3})$  above 30 K to  $\exp(A \cdot T^{-1/4})$  below. These correspond to variable range hopping of the carriers in two and three dimensions, respectively. Hence, the negative MR above 30 K is associated with two-dimensional transport in the  $\text{CuO}_2$  planes, whereas below 30 K, additional conduction between planes has a different, positive MR mechanism that dominates the bulk MR of ceramic samples. The correlation between low-temperature MR and mean cation radius in Figure 2 thus results from the decrease in the width of the insulating  $(R, \text{Ce})_2\text{O}_{2-\delta}$  slab between  $\text{CuO}_2$  planes as cation size decreases, leading to more three-dimensional conducting behavior in the small  $R$  materials.

In summary, the combination of electronically active  $\text{RuO}_2$  and  $\text{CuO}_2$  planes and a sophisticated chemical tuning from the  $(R, \text{Ce})_2\text{O}_{2-\delta}$  slabs leads to an exquisite variation of low-temperature conducting properties in  $\text{RuSr}_2(R_{2-x}\text{Ce}_x)\text{Cu}_2\text{O}_{10-\delta}$  materials. Low-doped, large  $R^{3+} = (\text{Nd}, \text{Y})$  materials show large negative MRs characteristic of two-dimensional magnetopolaron hopping, suppressed at higher dopings by superconducting pair formation. Analogues with small  $R = \text{Eu}$  or  $\text{Gd}$  have positive MRs associated with three-dimensional hopping, crossing over to negative MRs at high temperatures or fields. Superconducting materials with  $T_c$ 's up to 50 K can also be prepared using high  $R = \text{Sm}, \text{Eu}$ , or  $\text{Gd}$  contents.<sup>4,5,13,14</sup> Further studies of these materials may give new insights into superconducting and magnetoresistive electron transport in oxides, and could lead to improved oxide-based electronic devices.

**Acknowledgment.** We acknowledge The Royal Society of Edinburgh for a SEELLD research fellowship (A.C.M.), the Ministry of Science and Technology, Government of Pakistan for a studentship (F.S.), and the Leverhulme Trust and UK EPSRC for beam time provision and financial support.

**Supporting Information Available:** Table of  $\text{RuSr}_2\text{Nd}_{1.8-x}\text{Y}_{0.2}\text{Ce}_x\text{Cu}_2\text{O}_{10-\delta}$  compositions. This material is available free of charge via the Internet at <http://pubs.acs.org>.

## References

- (1) Reznik, D.; Pintschovius, L.; Ito, M.; Iikubo, S.; Sato, M.; Goka, H.; Fujita, M.; Yamada, K.; Gu, G. D.; Tranquada, J. M. *Nature* **2006**, *440*, 1170–1173.
- (2) McLaughlin, A. C.; Janowitz, V.; McAllister, J. A.; Attfield, J. P. *Chem. Commun.* **2000**, 1331–1332.
- (3) McLaughlin, A. C.; Janowitz, V.; McAllister, J. A.; Attfield, J. P. *J. Mater. Chem.* **2001**, *11*, 173–178.
- (4) Knee, C. S.; Rainford, B. D.; Weller, M. T. *J. Mater. Chem.* **2000**, *10*, 2445–2447.
- (5) McLaughlin, A. C.; Attfield, J. P.; Asaf, U.; Felner, I. *Phys. Rev. B* **2003**, *68*, 014503.
- (6) McLaughlin, A. C.; Sher, F.; Attfield, J. P. *Nature* **2005**, *436*, 829–832; McLaughlin, A. C.; Sher, F.; Attfield, J. P. *Nature* **2005**, *437*, 1057–1057.
- (7) Pelletted stoichiometric mixtures of  $\text{R}_2\text{O}_3$ ,  $\text{RuO}_2$ ,  $\text{CuO}$ ,  $\text{CeO}_2$ , and  $\text{SrCO}_3$  powders were sintered three times for 10 h in air at 1025 °C and cooled at 2 °C·min<sup>-1</sup>. Tetragonal  $I4/mmm$  1222 phases ( $a \approx 3.85 \text{ \AA}$ ,  $c \approx 28.55 \text{ \AA}$ ) were formed in all cases. All samples are semiconducting.
- (8) Williams, G. V. M.; Jang, L.-Y.; Liu, R. S. *Phys. Rev. B* **2002**, *65*, 064508.
- (9) Nagaev, E. L. *JETP Lett.* **1967**, *6*, 18–20.
- (10) Majumdar, P.; Littlewood, P. *Phys. Rev. Lett.* **1998**, *81*, 1314–1317.
- (11) Shannon, R. D. *Acta Crystallogr., Sect. A* **1976**, *32*, 751–767.
- (12) Parker, D. R.; Green, M. A.; Bramwell, S. T.; Wills, A. S.; Gardner, J. S.; Neumann, D. A. *J. Am. Chem. Soc.* **2004**, *126*, 2710–2711.
- (13) Ono, A. *Jpn. J. Appl. Phys.* **1995**, *34*, L1121.
- (14) Felner, I.; Asaf, U.; Levi, Y.; Millo, O. *Phys. Rev. B* **1997**, *55*, R3374–R3377.

JA064778H